CAAP Quarterly Report

June 30, 2025

Project Name: Enhancing Knowledge and Technology to Prevent and Mitigate Risks of Stress Corrosion Cracking (SCC) for Pipeline Integrity Management

Contract Number: 693JK32450002CAAP

Prime University: Stevens Institute of Technology

Prepared By: Yi Bao, yi.bao@stevens.edu, 201-216-5223

Reporting Period: [04/01/2025-06/30/2025]

Project Activities for Reporting Period:

During this quarter, we primarily focused on four tasks: (1) designing the experimental plan; (2) defining the specific experimental tasks; (3) revising the previous report and preparing two review papers; and (4) training student in the use of equipment.

According to Subtask II-1, the experimental plan primarily focuses on investigating the effects of individual factors on pipeline SCC. Based on comprehensive literature review and preliminary investigations, we have initially determined the ranges of individual causal factors. We will further discuss with consultants and the Technical Advisory Panel (TAP) to finalize the ranges of the factors. Additionally, we have refined the experimental procedures, including clarifying the specimen design, preparation methods, and testing protocols. We have started with small-scale specimens for material testing for two reasons: (1) small specimens allow us to efficiently investigate the basic effects of individual causal factors on SCC under controlled laboratory conditions, thereby laying a solid ground for subsequent large-scale experiments; and (2) small specimens help minimize sample preparation time and costs, allowing us to efficiently test more factors influencing pipeline SCC. Based on extensive experimental data for small-scale specimens, we will gain comprehensive understandings and then proceed to large-scale tests. In our tests, we conduct pre-loading to simulate the service loading conditions of pipelines prior to SCC initiation, followed by corrosion exposure and loading, and finally, slow strain rate testing (SSRT) to evaluate the environmentally assisted cracking (EAC) susceptibility of the steel.

During the corrosion exposure and loading process, we are employing ultrasonic testing (UT), acoustic emission (AE), fiber optic sensors, digital image correlation (DIC), X-ray micro-computed tomography (micro-CT), and scanning electron microscopy (SEM) to collect relevant data with the objectives of: (1) evaluating the effects and underlying mechanisms of individual factors on SCC, and establishing quantitative relations between these factors and SCC initiation time and growth rate; (2) evaluating the performance of existing techniques in terms of sensitivity and accuracy; (3) using UT and AE to develop cooperative multi-scale monitoring techniques; and (4) performing coupled multi-physics simulation and utilizing the experimental data to validate and refine these models, which will then be used to analyze the SCC mechanisms of the causal factors.

Regarding Subtask I from the previous quarter, we have revised the report and provided feedback on the suggestions raised by the project manager. In addition, we drafted and further improved two review papers. Currently, both papers are being reviewed by coauthored and will be submitted to journals for peer-review within July 2025. The two papers are tentatively titled "Review of Nondestructive Evaluation Techniques for Pipeline Stress Corrosion Cracking" and "A Review on Pipeline Stress Corrosion Cracking (SCC): Mechanisms, Causal Factors, Predictive Models, and Mitigation Strategies", respectively.

Regarding student training, Shengju Xie is receiving comprehensive trainings provided by the managers of the shared laboratories at Stevens Institute of Technology. The trainings are mandatory according to Stevens' latest lab safety policies, and the trainings cover general lab safety trainings and specialty trainings for the operation of various equipment such as SEM and micro-CT, as well as the procedures for handling chemicals. Yao Wang has received trainings on various nondestructive testing equipment such as UT, AE, and fiber optic sensors.

This report was jointly written and revised by three graduate students (Ms. Shengju Xie, Mr. Yao Wang, and Mr. Samuel Ajayi) under the guidance of four PI/co-PIs and one consultant. Shengju Xie was primarily responsible for the investigation of key experimental parameters, specimen design and preparation, and laboratory testing, with a focus on SCC mechanisms. Yao Wang concentrated on the experiments for AI-powered monitoring techniques. The main contents are summarized as follows:

1. Experimental parameters

The experimental design for investigating the effects of individual causal factors on SCC is shown in **Table 1**. The individual factors considered in this study include pressure cycling, temperature cycling, soil conditions, pipe grade, heat treatment, and welding. Following an extensive review of relevant literature, we established a preliminary set of parameters for these causal factors based on existing studies. However, several parameters, especially those related to pressure cycling, still require further refinement through consultation with industry partners to ensure practical relevance and applicability.

Table 1. Design of experimental for individual causal factors

Causal factor	Pressure cycling		Temperature cycling		Soil condition		Metallurgy		Welding method
	Amp.	Freq.	Amp.	Freq.	Concen.	pH	Grade	Treatment	
Control	PCA1	NA	TCA1	NA	C1	pH2	G1	T1	W1
Pressure cycling	PCA1 to PCA3	PCF1	TCA1	NA	C1	pH2	G1	T1	W1
Temperature cycling	PCA1	NA	TCA1 to TCA3	TCF1 to TCF3	C1	pH2	G1	T1	W1
Soil condition	PCA1	NA	TCA1	NA	C1 to C3	pH1 to pH3	G1	T1	W1
Pipe grade	PCA1	NA	TCA1	NA	C1	pH2	G1 to G3	T1	W1
Treatment	PCA1	NA	TCA1	NA	C1	pH2	G1	T1 to T3	W1
Welding	PCA1	NA	TCA1	NA	C1	pH2	G1	T1	W1 to W3

Note: Amp. = Amplitude, Freq. = Frequency, and Concen. = Concentration.

Steel grade. API 5L X65, X70, and X80 are the most widely used pipeline steels in both practical applications and academic research [1]. Accordingly, X65 (G1), X70 (G2), and X80 (G3) are selected for this project to investigate the effect of steel grade on SCC.

Welding methods. Low frequency electric resistance welding (W1), high-frequency electric resistance welding (W2), and submerged arc welding (W3) are selected for this project to investigate the effect of welding method on SCC.

Heat treatment. As rolled (T1), normalized + tempered (T2), and thermomechanical controlled process (T3) are selected for this project to investigate the effect of heat treatment method on SCC.

pH. Analysis of field samples indicated that cracking is most frequently associated with a solution pH of approximately 6.5 beneath damaged coatings [2]. Although the measured pH values may deviate from the actual values present at the crack sites, they still serve as useful references. In addition to the investigation of near-neutral pH SCC, pH values of 9 and 10 were also selected to represent high-pH SCC conditions. Accordingly, 6.5 (pH1), 9.0 (pH2), 10.0 (pH3) are selected for this project to investigate the effect of pH on SCC.

Temperature. According to reference [3], the operating temperature range of main gas pipelines is typically between 25 °C and 60 °C during summer and between -30 °C and 30 °C during winter. In this project, we test three temperatures to evaluate the influence of temperature on pipeline SCC, which are 25 °C (TCA1), 45 °C (TCA2), and 60 °C (TCA3). The room temperature is approximately 25 °C, and higher temperatures (45 °C and 60 °C) are achieved and maintained using a heating blanket.

Pressure cycling. To simulate the pressure cycling experienced by pipelines in service, pre-cyclic loading in air is conducted to treat the specimens. This process aims to introduce initial defects in the material. After defect formation, the specimens are submerged in a corrosive solution and periodically tested under cyclic loading. This approach is intended to replicate the combined effects of material defect, corrosion, and mechanical stress, which are key contributors to pipeline SCC. Then, SSRT will be conducted to evaluate the material's susceptibility to EAC.

(1) Pre-cyclic loading

To introduce microcracks into the new specimens, pre-cyclic loading has been performed in air. The loading scheme was designed based on field testing data in reference [4]. There are three loading blocks with varying ratios of the minimum stress to the maximum stress. This ratio is denoted by R, and its values are 0.9, 0.8, and 0.5, respectively. The number of load cycles are 25, 3, and 2, respectively. The maximum stress was 80% specified minimum yield strength (SMYS). A constant strain rate of 50 με/s is applied to the pre-cyclic loading. A total of 8000 cycles is applied to simulate the stress cycling experienced by pipelines over 20 years of service. The pre-cycling loading scheme is shown in **Fig. 1**.

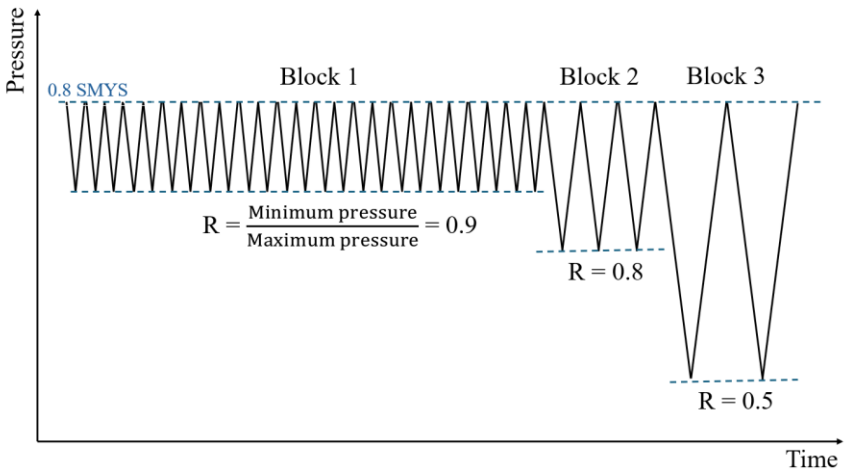

Fig. 1. Simplified pre-cycling loading scheme [4].

(2) Post corrosion exposure cycling loading

As shown in **Fig. 2**, the actual pressure cycling experienced by in-service pipelines exhibits time-dependent variations in both amplitude and frequency. However, accurately replicating such complex pressure fluctuation patterns in a laboratory environment presents significant challenges. Therefore, this study adopts constant-amplitude cyclic loading as an initial experimental approach, aiming to systematically evaluate the effects of loading amplitude and frequency on the susceptibility of pipeline steel to SCC. It is worth noting that both loading amplitude and frequency are intrinsically related to the applied strain rate.

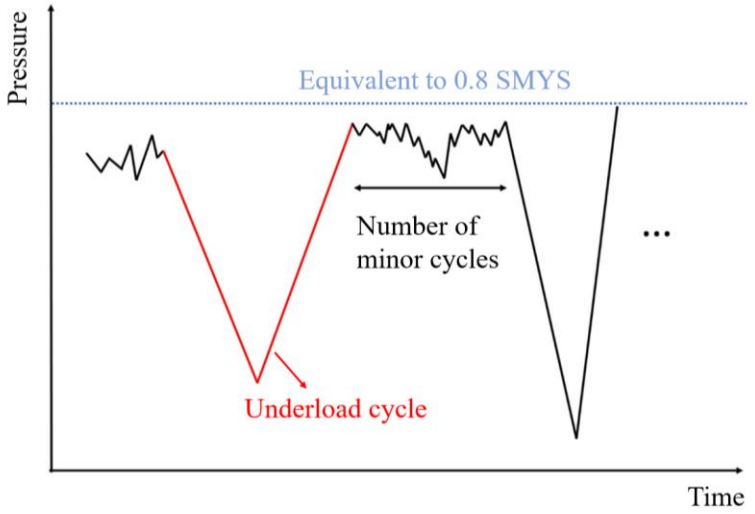

Fig. 2. Actual pressure cycling experienced by in-service pipelines [5].

According to the standard of B31.4 and B31.8, the allowable stresses in pipelines can be expressed as [6,7]:

$$S = F \times E \times S_y \tag{1}$$

where S is the allowable stress; E is weld joint factor; F is design factor based on nominal wall thickness, typically equal to 0.72; and S_y is the SMYS of the pipe material.

Accordingly, the baseline pressure cycling amplitude (PCA1) is conservatively set at 0.8×SMYS, with PCA2 and PCA3 set at 0.7×SMYS and 0.9×SMYS, respectively. In addition, the pressure cycling frequency is initially set at 5×10^{-3} for PCF1, 5×10^{-2} for PCF2, and 5×10^{-4} for PCF3, respectively.

(3) SSRT

After the pre-cyclic loading in air and cyclic loading under corrosion exposure, SSRT is conducted to evaluate the steel's susceptibility to EAC. The strain rate for SSRT is preliminary set at 1 με/s according to the recommendations of ASTM G129 [8] and ISO 7539-7 [9].

2. Specimen design

Although small specimens are typically used in SCC mechanism studies and SSRT tests, this study aims to address both the investigation of SCC mechanisms and the integration of crack monitoring equipment (AE technology). Therefore, the specimen design must accommodate AE sensor installation while ensuring reliable SCC evaluation. ASTM E8 specifies standard tensile specimens (**Fig. 3**) for large-diameter tubular products, and noted that the G/W ratio should exceed 4 for accurate elongation measurements. Since elongation is a critical indicator for evaluating EAC susceptibility in SSRT tests, selecting appropriate specimen geometry is essential to obtain valid results. The preliminary specimen dimensions are listed in **Table 2**. To ensure secure gripping during testing and minimize unnecessary exposure to the corrosive environment, the central section of the specimen will serve as the focus area for SCC evaluation, with the remaining sections protected during testing. We plan to replace dog-bone specimens with coupon specimens. The standards do not impose specific limitations on the specimen dimensions. As long as the specimens can be securely gripped in the loading equipment without affecting the stress distribution in the gauge area, the impact of specimen shape on experimental results will be minimal. Currently, each experimental set includes three specimens. We may further adjust the dimensions and quantity of specimens according to preliminary testing results.

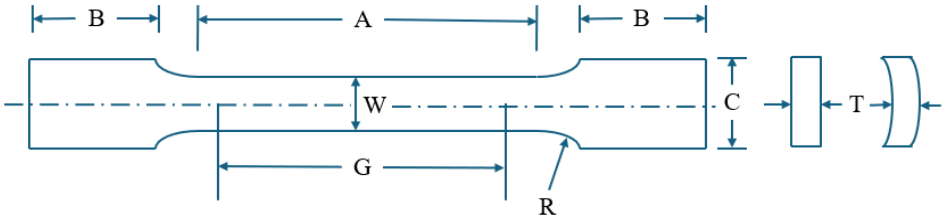

Fig. 3. Tension test specimens dimension for large diameter tubular products [10].

Table 2. Dimensions of the specimen

Parameter	Symbol	Value
Gage length	G	100 mm
Width	W	20 mm
Thickness	T	NA
Radius of fillet	R	25 mm
Length of grip section	A	120 mm
Length of grip section	B	75 mm
Width of grip section	C	25 mm

3. Solution preparation

Based on literature review, the preliminary preparation methods for the corrosion solutions are as follows:

Near neutral pH solution. Before the test, the solution needs to be purged with 5% CO_2 gas that was balanced with N_2 for a period of 2 hours to establish a near neutral pH. The composition of the NS4 solution, prepared using analytical-grade reagents and deionized water (pH = 7), is shown in **Table 3** [11,12].

Table 3. Chemical composition of NS_4 solution

Chemicals	KCl	$CaCl_2 \cdot 2H_2O$	$NaHCO_3$	$MgSO_4 \cdot 7H_2O$
Concentrations (mg/L)	122	181	483	131

High pH solution. References [5,13,14] recommended that a standard solution for high-pH SCC laboratory experiments consists of an aqueous solution containing 0.5 M Na_2CO_3 and 1 M $NaHCO_3$.

4. Facilities, equipment, and materials

We have access to necessary facilities, equipment, chemicals, and sensors to support solution preparation, specimen treatment and testing, crack monitoring, and examination of specimens with SCC. Additionally, dog-bone specimens have been prepared for preliminary experimental evaluation. Furthermore, certain items, including AE equipment with compatible sensors and gases for pH balancing, are currently on the way.

4.1 Existing facilities, equipment and sensors

The facilities and major equipment that we are using or will be using include, but are not limited to, MTS material test system, SEM, X-ray micro-CT, UT system, piezo ceramic plate, fume hood, glove box, pH meter, and precision balance. They are briefly presented as follows.

(a) MTS material test system (**Fig. 4**). Load capacity: dynamic (100 kN); static (120 kN). With load cells and extensometers embedded.

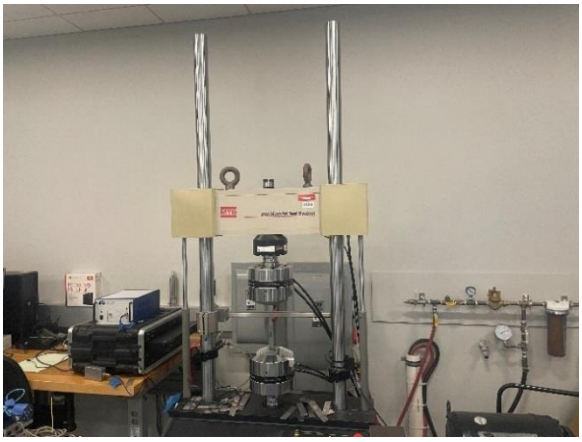

Fig. 4. MTS material test system.

(b) Scanning electron microscopy: Zeiss Auriga FIB/SEM (**Fig. 5**). The system provides a resolution of 1.0 nm at 15 kV and 1.9 nm at 1 kV, with a magnification range of 12x to 1000 kx and an adjustable probe current of 4 pA to 20 nA.

Fig. 5. Zeiss Auriga FIB/SEM.

(c) Desk-top X-ray microtomography: Skyscan 1272 (**Fig. 6**). The micro-CT system is equipped with an X-ray source operating at 40-100 kV with a power of 10 W, achieving a spot size of less than 5 μm at 4 W. It features a 16 MP sCMOS detector (4096×4096 pixels) for high-resolution imaging. The system accommodates objects with a maximum diameter of 75 mm and a height of up to 80 mm.

Fig. 6. Skyscan 1272.

(d) UT system (**Fig. 7**). Waveform generator: Keysight 33500B. Supporting sine and pulse outputs up to 30 MHz, with a jitter of less than 40 ps. It offers an amplitude range from 1 mVpp to 10 Vpp, a 250 MSa/s sampling rate, 16-bit amplitude resolution, and 1 MSa/channel memory. Wideband power amplifier: Krohn-Hite 7602M. Delivering up to 17 W or 34 W output power, with corresponding output voltages of 141 V and 282 V rms. It operates over a frequency range from DC to 1 MHz, with selectable AC or DC coupling, and provides gain up to 42 dB. The total harmonic distortion is less than 0.01%. Oscilloscope: Keysight DSOX3014T. Featuring 4 analog input channels, 100 MHz bandwidth, and 4 Mpts memory depth. It offers a waveform update rate of up to 1 million waveforms per second and supports standard touch zone triggering via an 8.5 inch capacitive touch screen.

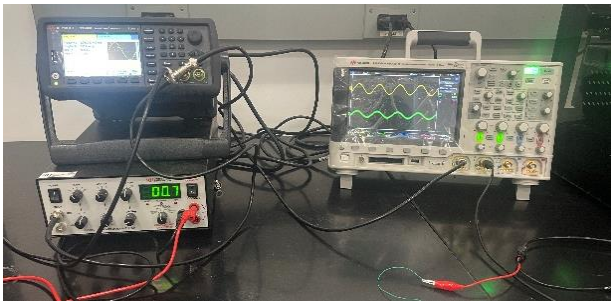

Fig. 7. Ultrasonic testing system.

(e) Piezo ceramic plate: 26×16×0.7 mm, 108 kHz (**Fig. 8**). The electromechanical coupling coefficient (K_{31}) exceeds 41%, and the resonant impedance (Z_m) is smaller than 18 Ω. The static capacitance (C_s) is 6800 ± 15% pF, measured at 1 kHz.

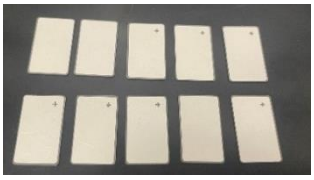

Fig. 8. Piezo ceramic plate.

(f) Piezo ceramic plate: 7×8×0.2 mm, wire lead, 240 kHz (**Fig. 9**). The electromechanical coupling coefficient (K_{31}) exceeds 40%, and the resonant impedance (Z_m) is smaller than 2 Ω. The static capacitance (C_s) is 3300 ± 10% pF.

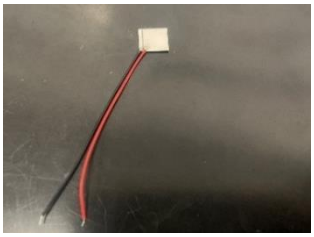

Fig. 9. Piezo ceramic plate.

(g) Fume hood (**Fig. 10**). This fume hood is designed for use with substances that produce hazardous levels of airborne chemicals, including gases, fumes, vapors, aerosols, and dust.

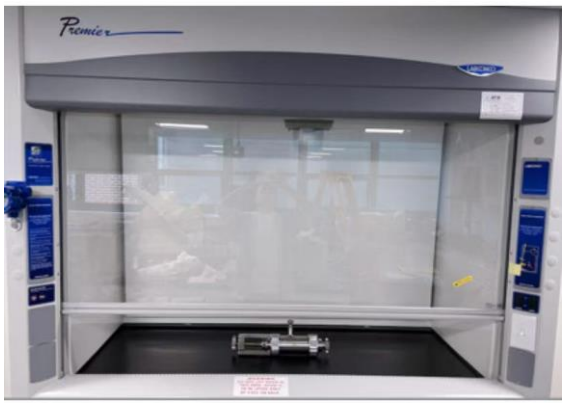

Fig. 10. Fume hood.

(i) pH meter (**Fig. 11**): with a precision of 0.01 and temperature measurement function.

Fig. 11. pH meter.

(j) Precision balance (**Fig. 12**): with a precision of 0.001g.

Fig. 12. Precision balance.

4.2 Chemicals

We have procured and received chemical reagents for preparing corrosion solutions (**Fig. 13**), which include $NaHCO_3$, $CaCl_2 \cdot 2H_2O$, $MgSO_4 \cdot 7H_2O$, KCl, NaOH, and Glacial acetic acid.

Fig. 13. Chemicals for preparing corrosion solutions.

4.3 Dog-bone specimen

Dog-bone specimens have been prepared for preliminary experiments (**Fig. 14**). The dog-bone specimens were cut from steel pipes measuring 1830 mm in length, 115 mm in outer diameter, and 6 mm in wall thickness.

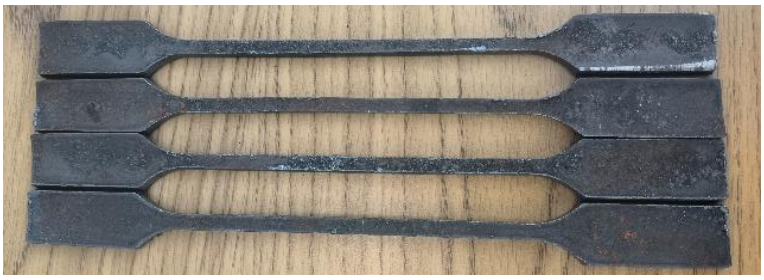

(a)

(b)

Fig. 14. Dog-bone specimens: (a) a photo of representative specimens, and (b) positions of the specimens in the pipes.

4.4 Procurement in progress

The following items have been ordered and shipped:

(a) EasyAE with communication cables (USB3 and USBC) and factory case.

(b) R15A Sensor, Alpha series, 150 kHz, SMA connector.

(c) Gas cylinder: 5% CO_2 balanced with N_2 for solution pH balance.

5. Experimental procedures

To investigate the effects of individual causal factors on the mechanism of SCC, the experimental procedures have been further refined in accordance with ASTM G129 [8] and ASTM E8/E8M [10]. Research variables, control variables, and specimen quantities have been explicitly defined to ensure the scientific rigor and reproducibility of the experimental process. Experimental groups have been established for each variable to enable clear identification of the effects of single-factor variations on SCC behavior, while other potential influencing factors are rigorously controlled to maintain data accuracy and comparability. This systematic experimental design aims to comprehensively clarify the roles of specific causal factors in SCC mechanisms and to generate reliable data for subsequent mechanistic analyses and model development.

5.1 Effect of pressure cycling on SCC

The design for testing the effect of constant amplitude loading on SCC is shown in **Table 4**. The experimental procedure is as follows:

(a) Since the specimen is not pre-cracked, the time instant when cracking initiates under corrosion and loading conditions are uncertain. Therefore, a preliminary test of corrosion and mechanical loading is necessary to determine the onset of cracking.

(b) Specimen preparation should ensure that the surface finishes meet the applicable standards. Test specimens must be degreased and cleaned prior to testing, and care should be

taken to avoid contamination before the test. Gauge marks and speckle patterns should be prepared to enable observation of crack development in the exposed corrosion area during cyclic loading using DIC techniques, and to facilitate elongation measurements during SSRT. Weigh the specimen to obtain its initial weight. Measure the cross-sectional area of the specimen.

(c) Pre-cyclic loading is conducted with the specimen gripped in the loading machine.

(d) The grip sections of the specimen are protected using epoxy resin or other suitable measures, leaving only the central gauge area exposed for subsequent immersion and cyclic loading. Simultaneously, AE sensors are installed for monitoring during the test. A simplified layout is shown in **Fig. 15**.

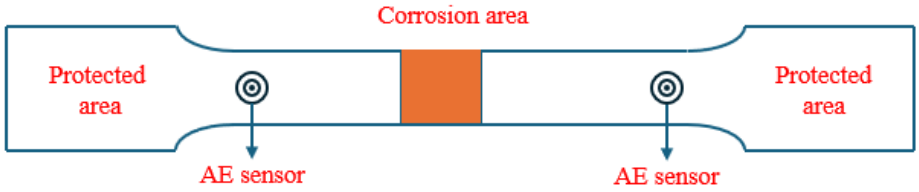

Fig. 15. Simplified layout of specimen and AE sensor positioning.

(e) The specimen is submerged in the corrosive solution and subsequently removed for post-exposure cyclic loading. It is loaded to the maximum stress amplitude and then unloaded. Relevant parameters are shown in **Table 4**. During the loading process, the DIC will be used to monitor the crack location, as well as the surface length and width of the cracks. The AE sensors are used to collect the cracking signal.

Table 4. Design for testing the effect of constant amplitude loading on SCC

Variables	Amplitudes	R	Frequency (Hz)	Number of specimens	Other parameters
None-corroded specimen for AE testing	0.8 × SMYS	0.5	5×10^{-3}	3	Steel grade: X65 Temperature: 25 °C Heat treatment: T1
Pressure cyclic amplitude	0.8 × SMYS	0.5	5×10^{-3}	3*	pH = 6.5 Steel grade: X65 Temperature: 25 °C Heat treatment: T1
	0.7 × SMYS			3	
	0.9 × SMYS			3	
Pressure cyclic frequency	0.8 × SMYS	0.5	5×10^{-2}	3	
			5×10^{-3}	3*	
			5×10^{-4}	3	
R-ratio	0.8 × SMYS	0.5	5×10^{-3}	3*	
		0.8		3	
		0.9		3	

Note: "*" denotes the control condition; A total of 24 specimens have been counted in this table.

It remains unclear whether the corrosion products on the steel surface affect the performance of DIC techniques. If the presence of corrosion products compromises the accuracy of crack length and width measurements, it may be necessary to remove the corrosion products before conducting this loading and crack monitoring step.

(f) After the loading process, non-destructive testing techniques such as UT are used to measure crack depth.

(g) Repeat steps (e) and (f).

(h) After a specified number of exposures and loading cycles, the specimens undergo SSRT to evaluate the susceptibility to EAC.

(i) Finally, the specimens are cleaned, weighed, and examined to assess the pitting corrosion condition and distribution. Then, the specimens are sectioned for further analysis. SEM and micro-CT are performed to examine the fracture surface morphology and microstructural features to determine the crack propagation mode (e.g., intergranular or transgranular fracture, brittle or ductile fracture, and hydrogen embrittlement).

5.2 Effect of temperature on SCC

The design for testing the effect of temperature and temperature cycling on SCC is shown in **Table 5**. The experimental procedure is similar to that described in Section 5.1, with adjustments made only to the immersion solution temperature as required.

Table 5. Design for testing the effect of temperature on SCC

Variable		Number of specimens	Other parameters
Constant temperature	25 °C	3*	pH =6.5 Steel grade: X65 Heat treatment: T1 Cyclic loading amplitude: 0.8 × SMYS Cyclic loading frequency: 5×10^{-3} R: 0.5
	45 °C	3	
	60 °C	3	
Cyclic temperature	Amp.: 25-60 °C	3	
	Period = 1 day		

Note: "*" denotes the control condition. Since the control condition is the same as that in **Table 4**, 9 specimens are added.

5.3 Effect of soil condition, steel grade, and heat treatment on SCC

The design for testing the effect of soil condition, steel grade, and heat treatment on SCC is shown in **Table 6**. The experimental procedure is similar to that described in Section 5.1, with adjustments made as needed to the immersion solution pH or to the specific specimens used.

Table 6. Design for testing the effect of soil condition, steel grade, and heat treatment on SCC

Variable	pH	Steel grade	Heat treatment	Number of specimens	Other parameters
Effects of pH	6.5	X65	T1	3*	Temperature: 25 °C Cyclic loading amplitude: 0.8 × SMYS Cyclic loading frequency: 5×10^{-3} R: 0.5
	9.0			3	
	10.0			3	
Effects of steel grade	6.5	X65	T1	3*	
		X70		3	
		X80		3	
Effects of heat treatment method	6.5	X65	T1	3*	
			T2	3	
			T3	3	
Effects of welding method	6.5	X65	T1	3	
				3	
				3	

Note: "*" denotes the control condition. Since the control condition is the same as that in **Table 4** and **Table 5**, 27 specimens are added.

5.4 Monitoring of the development of SCC using acoustic emission

This study aims to monitor the real-time development of SCC using AE techniques during the loading test. The sensors are attached to the specimen with corrosive production to capture transient elastic waves generated during crack initiation and propagation under mechanical

loading. Throughout the entire loading process, AE signals are continuously recorded. By analyzing signal parameters such as amplitude, frequency, and energy, the progression of SCC can be tracked and characterized. The objective is to extract AE features indicative of different cracking stages, thereby enabling early detection and understanding of pipeline SCC behavior. The experimental procedure is as follows:

(a) Label each dog-bone specimen, record condition, especially the corrosion-loading cycle.

(b) Clean the surface to ensure good coupling between sensors and specimens.

(c) Attach two identical R15α sensors symmetrically on the surfaces of the shoulder regions at both ends of the specimen's gauge section.

(d) Evaluate the coupling quality and response consistency of AE monitoring system using the pencil lead break (PLB) method as a simulated signal source prior to formal testing.

(e) Determine the signal detection threshold based on the ambient noise level recorded under testing conditions.

(f) Monitor and record AE signals to capture crack initiation and propagation events in real time during the loading process.

(g) Analyze the recorded AE data to extract key parameters such as hits, amplitude, energy, and rising time.

5.5 Detecting of SCC using ultrasonic testing

This study aims to differentiate the wave propagation characteristics among undamaged specimens, those with conventional tensile damage, and those with SCC. To understand the specific ultrasonic responses caused by SCC, the identical dog-bone samples that are simply broken by tensile fracture will also be detected. During the test, Lead Zirconate Titanate (PZT) transducers are first mounted on both ends of the specimen using conductive epoxy before the corrosion process begins. The mounted transducers are then protected with corrosion-resistant materials such as heat shrink tubing. After each corrosion-loading cycle, UT is performed to determine whether cracks have initiated and to analyze the ultrasonic responses. By comparing the UT signal responses from three groups, including intact samples, the SCC-damaged samples, and the tensile-fractured samples, clear acoustic differences between different damages can help distinguish SCC from simple mechanical damages. The experimental procedure is as follows:

(a) Label each dog-bone specimen, record condition, especially the corrosion-loading cycle.

(b) Clean the surface to ensure good coupling between PZT and specimen.

(c) Attach the PZT transducers to the specimen using thermally conductive epoxy, assigning them as transmitter and receiver, respectively.

(d) Protect the PZT sensors using heat shrink tubing and anti-corrosion measures to prevent interference from the corrosion testing environment.

(e) Adjust instrument settings based on dispersion analysis.

(f) Pitch-catch will be used to detect the specimens.

(g) Acquire ultrasonic waveform data and analyze the key parameters.

6 Experimental equipment training

To ensure the smooth execution of the experimental tasks and to protect the personal safety of all participants, experimental equipment training was conducted during this period. The training primarily covered the use of the MTS loading system, DIC, micro-CT, and UT systems.

During the ultrasonic non-destructive testing training, dispersion analysis and guided wave detection were trained. A preliminary dispersion analysis was performed based on existing steel pipes in our laboratory to determine the ultrasonic excitation frequency and select an appropriate transducer. The pipe has an outer diameter of 115 mm, a thickness of 6 mm, and a length of 1,830 mm. Selection of the excitation frequency and wave mode is guided by a detailed analysis of the dispersion curves for various wave modes. These dispersion curves were generated using an open-source tool called *Dispersion Calculator*. The phase velocities of various wave modes over a range of frequencies are shown in **Fig. 16(a)**. To minimize signal analysis complexity, the L(0, 2) mode within 30-200 kHz was preliminarily selected, as it exhibits nearly constant phase velocity, indicating low dispersion and consistent propagation behavior. The corresponding energy velocities are presented in **Fig. 16(b)**, where the L(0, 2) mode displays a distinct energy velocity compared to coexisting longitudinal modes. In experiments, this mode typically appears as the first wave in the transmitted signal. Prior to the formal testing, material characterization of the samples will be performed, followed by a comprehensive dispersion analysis to guide the optimization of guided wave excitation.

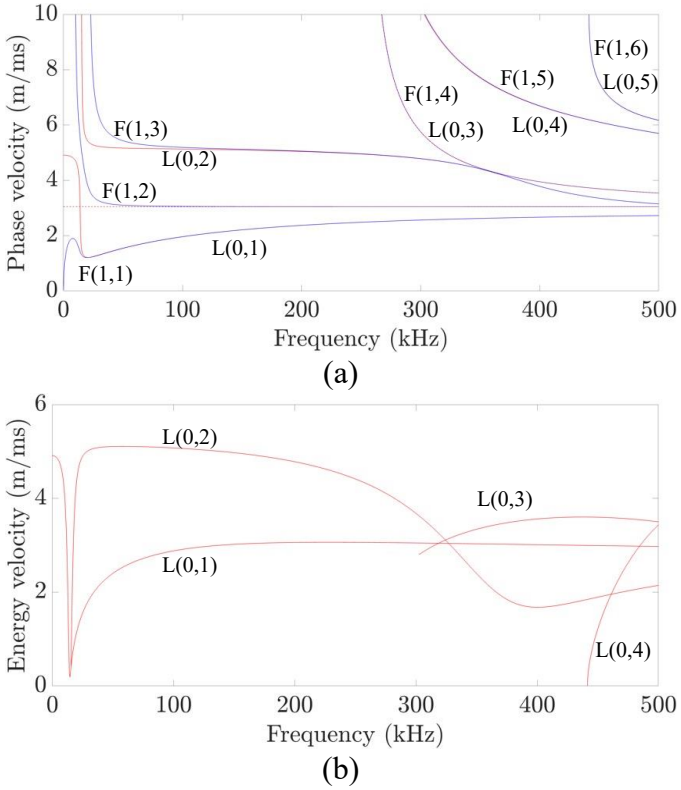

Fig. 16. Dispersion curves of the pipe specimen: (a) phase velocity, and (b) energy velocity.

In addition, we have conducted preliminary training with the UT system. This included PZT installation and operation of the UT system (**Fig. 17**). Using the waveform generator, we tested

both sine waves and tone burst signals on aluminum plates. This training will facilitate smoother installation and testing procedures in the upcoming formal experiments.

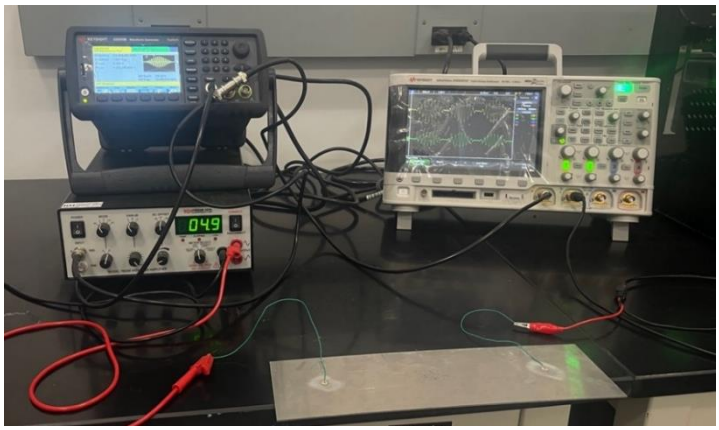

Fig. 17. Preliminary training in ultrasonic testing.

Project Financial Activities Incurred during the Reporting Period:

The Prime university (Stevens Institute of Technology) fully executed the agreement with the PHMSA and sub-universities (North Dakota State University and Rutgers University).

Project Activities with Cost Share Partners:

There were no major activities that were conducted during this reporting period with cost share partners.

Project Activities with External Partners:

The primary activities that were conducted during this reporting period with external partners or sub-universities include: (1) collaborative effort for the literature review task (Task I); (2) discuss and finalize the preliminary testing plan and equipment procurement (Task II); and (3) experimental equipment training (Task II).

Potential Project Risks:

We have not identified major projects risks. The project is progressing as planned.

Future Project Work:

In the next 30 days, we will conduct preliminary single-factor SCC tests to evaluate the compatibility and coordination of different experimental setups and instruments. Based on the preliminary test, the testing protocol will be refined accordingly. In the next 60 days, we aim to conduct formal experiments and collect results based on experiment plan and Task II. In the next 90 days, we plan to analyze the results of single-factor SCC experiments and write a research paper. We will also conduct numerical simulation of detecting damage using guided waves to expand the datasets.

Potential Impacts on Pipeline Safety:

There are four main impacts: (1) *Improved Understanding of SCC Mechanisms*: The literature review enhances the understanding of SCC mechanisms, including the roles of metallurgical defects, environmental variables, and pipeline stresses. This knowledge contributes

to better design experiments for investigating the effects of casual factors of pipeline SCC under various operational and environmental conditions. Insights from reviewed studies on SCC in high-pH, near-neutral pH, and acidic environments directly support the development of effective risk mitigation measures. (2) *Identification of Knowledge Gaps*: By summarizing existing gaps, such as limited understanding of coupled factors (e.g., temperature and pressure cycling), long-term SCC behavior, and the mechanism of variable pressure fluctuation, the project provides a roadmap for targeted research. (3) *Enhancement of Monitoring Techniques*: The review of nondestructive SCC monitoring methods summarizes the applicable scenarios, strengths, and weaknesses of mainstream monitoring technologies. The evaluation and comparison help in selecting appropriate techniques for practical applications based on different scenarios. Meanwhile, by highlighting the weaknesses of existing methods (e.g., limited to surface crack, ineffectiveness in micro-scale crack), the project identifies opportunities for innovative technologies. (4) *Collaborative Efforts for Timely Risk Mitigation*. The biweekly discussions ensure that potential risks, such as delays in the project timeline or test-bed preparation, are monitored and mitigated proactively. This collaborative approach strengthens the project's capacity to maintain alignment with safety-critical milestones and deliver timely recommendations for industry adoption. (5) *Foundation for Advanced Research and Application*: The recruitment of graduate students and initial research efforts provide the human capital and knowledge base needed for subsequent project phases, including experimental studies and advanced risk models. This supports the development of unified safety models for pipelines and long-term improvement in pipeline integrity management practices.

References

[1] Abubakar, S.A., Mori, S. and Sumner, J., 2022. A review of factors affecting SCC initiation and propagation in pipeline carbon steels. Metals, 12(8), p.1397.

[2] Parkins, R.N., Blanchard, W.K. and Delanty, B.S., 1994. Transgranular stress corrosion cracking of high-pressure pipelines in contact with solutions of near neutral pH. Corrosion, 50(05).

[3] Nazarova, M.N., Akhmetov, R.R. and Krainov, S.A., 2017, October. Temperature factors effect on occurrence of stress corrosion cracking of main gas pipeline. In IOP Conference Series: Earth and Environmental Science (Vol. 87, No. 6, p. 062011). IOP Publishing.

[4] Wang, S.H., Chen, W., King, F., Jack, T.R. and Fessler, R.R., 2002. Precyclic-loading-induced stress corrosion cracking of pipeline steels in a near-neutral-pH soil environment. Corrosion, 58(6), pp.526-534.

[5] Niazi, H., Chevil, K., Gamboa, E., Lamborn, L., Chen, W. and Zhang, H., 2020. Effects of loading spectra on high pH crack growth behavior of X65 pipeline steel. Corrosion, 76(6), pp.601-615.

[6] ASME B31. 4, 2016. Pipeline transportation systems for liquids and slurries.

[7] American National Standards Institute, 1995. Gas transmission and distribution piping systems. American Society of Mechanical Engineers.

[8] ASTM G129-00 (2013), 2013. Slow Strain Rate Testing to Evaluate the Susceptibility of Metallic Materials to Environmentally Assisted Cracking. West Conshohocken, PA: ASTM.

[9] ISO 7539-7: 2005 (last reviewed 2014), 2005. Corrosion of Metals and Alloys-Stress Corrosion Testing-Part 7: Method for Slow Strain Rate Testing.

[10] ASTM E8/E8M, 2022. Standard Test Methods for Tension Testing of Metallic Materials.

[11] Luo, J., Luo, S., Li, L., Zhang, L., Wu, G. and Zhu, L., 2019. Stress corrosion cracking behavior of X90 pipeline steel and its weld joint at different applied potentials in near-neutral solutions. Natural Gas Industry B, 6(2), pp.138-144.

[12] Nking'wa, A.A. and Gao, K., 2024. Study on Stress Corrosion Cracking of X100 Pipeline Steel in NS4 Solution. Journal of Failure Analysis and Prevention, 24(4), pp.1934-1944.

[13] Niazi, H., Eadie, R., Chen, W. and Zhang, H., 2021. High pH stress corrosion cracking initiation and crack evolution in buried steel pipelines: A review. Engineering Failure Analysis, 120, p.105013.

[14] Lu, B.T., 2014. Further study on crack growth model of buried pipelines exposed to concentrated carbonate–bicarbonate solution. Engineering Fracture Mechanics, 131, pp.296-314.